ORIGINAL PAPER

Source Apportionment and Ecological-Health Risks Assessment of Heavy Metals in Topsoil Near a Factory, Central China

Jia Li[1,2] · Guangcai Wang[1,2] · Fei Liu[1,2] · Linfeng Cui[1,2] · Yanjun Jiao[1,2]

Abstract

Soil heavy metals pollution caused by industrial activities poses a great threat to the environment and human health and has become an increasingly concern worldwide. In this study, heavy metals/metalloid (Pb, As, Zn, Cu, Cr, Ni, Fe, Mn) in the topsoil around a factory, central China were investigated to identify their sources and to assess the potential ecological-health risks. A total of 106 soil samples were collected and analyzed in the study area. Statistical analysis and Positive Matrix Factorization (PMF) model revealed that Pb, As, Zn and Cu were main contaminants in the topsoil of the study area, which mainly originated from three sources: industrial fume emitted by factory entering the soil through dry deposition (41.3%), natural sources (52.1%), and sewage leakage (6.6%). Self-Organizing Map (SOM) indicated that the sampling sites could be grouped into four clusters. Potential ecological and human health risks were evaluated for each cluster. It was found that the potential ecological risks and the non-carcinogenic risks were relatively high in the southeast of the factory due to the soil pollution associated with the main wind direction, and the carcinogenic risks were relatively high in the northeast of the factory affected by the discharge of As-containing wastewater. The high-risk areas identified in this study could provide a priority for future control and treatment of heavy metals pollution.

Keywords Heavy metals · Source apportionment · Self-Organizing Map · Risks assessment

Introduction

With the rapid development of industrialization and urbanization, heavy metals pollution in soil has attracted extensive attention and research (Zhang et al. 2018a; Dong et al. 2019; Baitas et al. 2020; Liu et al. 2020; Wen et al. 2020). Heavy metals can migrate into groundwater and are absorbed by plants into the food chain, which causes a threat to ecosystems and human health (Zhu et al. 2012; Dai et al. 2014; Burges et al. 2015; Yuswir et al. 2015; Shang et al. 2016).

✉ Guangcai Wang
wanggc@pku.edu.cn

[1] State Key Laboratory of Biogeology and Environmental Geology & MOE Key Laboratory of Groundwater Circulation and Environment Evolution, China University of Geosciences, Beijing, China

[2] School of Water Resources and Environment, China University of Geosciences, Beijing, China

Lead, for example, may cause anemia, kidney disease, gastrointestinal colic, and central nervous system diseases (Pareja-Carrera et al. 2014). Arsenic may cause skin lesions, skin cancer and vascular disease (Tchounwou et al. 2012; Tan et al. 2016; Xiao et al. 2017). Although arsenic is a metalloid not a metal, it is often grouped with heavy metals in ecological-health risks studies (Zhang et al. 2018a; Wang et al. 2019b; Liu et al. 2020). In addition, even the metal elements required by the human body, if overexposed, will damage the health. For example, excessive copper will cause metabolism disorders, and even lead to liver cirrhosis (Ameh and Sayes 2019). Therefore, it is important to figure out the harmful effects of heavy metals pollution on ecosystems and human health (Dai et al. 2012; Huang et al. 2018a). Previous studies have found that heavy metals pollution is serious in population-intensive areas (Gülten 2011; Cai et al. 2019; Li and Jia 2018; Shi et al. 2019; Ye et al. 2019), especially in the vicinity of industrial areas (Harvey et al. 2017; Li et al. 2018; Lü et al. 2018; Zhang et al. 2018b; Antoniadis et al. 2019; Zhou and Wang 2019), which may have serious negative effects on ecosystems and human health (Machender

et al. 2011; Xue et al. 2014; Qing et al. 2015; Wu et al. 2018a).

Soil parent material itself contains a certain amount of heavy metals, so it is necessary to identify whether the sources of heavy metals are natural or anthropogenic. Receptor models can be used in the quantitative analysis of pollution sources. Commonly used receptor models are: Chemical Mass Balance (CMB) (Zheng et al. 2005), Positive Matrix Factorization (PMF) (Hu et al. 2018), UNMIX (Lang et al. 2015) and Factor Analysis-Multiple Regression Model (FA-MLR) (Pekey et al. 2004). Among them, PMF model showed an advantage in dealing with the missing data, error estimate, and contribution rate of each source at each sampling site, which makes it widely used in source apportionment (Jang et al. 2013; Kim et al. 2018; Men et al. 2018a; Li et al. 2019; Su et al. 2019; Zanotti et al. 2019; Cheng et al. 2020).

Soil heavy metals data are often complex, in order to accurately explain the relationship between the variables, it is usually necessary to reduce the dimensions and classify the data. Traditional dimensionality reduction and classification methods such as PCA and HA (Pathak et al. 2013; Li et al. 2014; Lu et al. 2017) sometimes fail to accurately identify the relationships between variables, which leads to misinterpretations, and they are not useful for the visual assessment of the results (Astel et al. 2007; Lischeid 2009; Wongravee et al. 2010). To overcome the shortcomings of traditional methods, Self-Organizing Map (SOM) has been increasingly used to classify data (Han et al. 2016; Tao et al. 2017; Nakagawa et al. 2020; Zhu et al. 2020). SOM is a powerful non-linear projection tool that visualizes complex high-dimensional data structures onto two-dimensional surfaces by organizing input data into a smaller number of neurons (Kohonen 1982). SOM can reveal local relationships between variables and can be used to classify widely dispersed data (Hong and Rosen 2001). In addition, SOM supports techniques that use the reference vectors to give an informative picture of the data, which can clearly demonstrate the interdependence of variables (Skwarzec et al. 2009; Pearce et al. 2011; Zelazny et al. 2011). This study tried to combine SOM with potential ecological-health risks assessment to help to identify the high-risk areas to protect the ecosystem and human health reasonably and efficiently.

A previous reconnaissance survey showed that the concentrations of some heavy metals, such as Pb, As, Zn, Cu, were relatively high in topsoil around a lead plant, central China, so the potential soil pollution in the area has become a great concern. The purpose of this study is to evaluate the soil pollution level, identify sources of heavy metals in the topsoil and calculate potential ecological-health risks in the area. The sources of heavy metals were analyzed by PMF model. After using SOM to cluster the data, the ecological-health risks caused by heavy metals were assessed

combining the SOM results, and the high risks areas around the factory were identified.

Materials and Methods

Study Area

The study area is around a lead smelting factory, central China, covering an area of approximately 25 km^2 (Fig. 1). It is located in a plain area and the terrain is flat with an altitude of 140.83–141.50 m. The study area is temperate continental monsoon climate, with an annual average temperature of 14.5 ℃ and an annual average rainfall of 568 mm. The study area is divided into three zones (residential land, commercial land and farmland). Approximately 800 people live in the east of the factory, and most of them are farmers, so we regarded this area as the residential zone. There are some little shops and supermarkets near the factory for the daily needs of workers and farmers, so we regarded them as commercial zone. The other area was covered by agricultural land, so we regarded it as farmland zone. The soils in the study area are mainly loam and sandy loam. The bulk density of topsoil is 1.48 g cm^{-3}. The soil development based on the parent material of Malan loess, and the leaching and deposition of calcareous substances are relatively weak, so the hierarchical differentiation of soil is not significant, and the soil color, texture, organic matter content and acidity and alkalinity of the core soil layer are relatively uniform (Wang et al. 2019a).

The factory was built in 1997, and mainly deals in the smelting of lead. Lead ore mixed with limestone and quartz sand was fed into the oxygen bottom blowing furnace to produce crude lead, accompanying liquid lead slag and dust fume. The crude lead was sent to the refiner, and the lead slag was mixed with stone and coke particles and then put into the reduction furnace for reduction, and dusty flue gas was sent to the acid-making system. The raw materials used in this plant was lead–zinc mineral, so zinc, copper and arsenic are common impurities. Therefore, these four elements become the focus of topsoil heavy metals pollution in the study area.

Soil Sampling and Analyses

Sampling sites were distributed around the factory, and a total of 106 soil samples were collected, and each sample was a mixture of five random subsamples taken from the upper soil horizon (0 to 20 cm) of the 1 × 1 km grid, and the sampling sites were dense near the factory and distributed radially with the factory as the center (CEPA 2004). The original weight of each soil sample was greater than 1000 g. All samples were stored in a polyethylene package to avoid
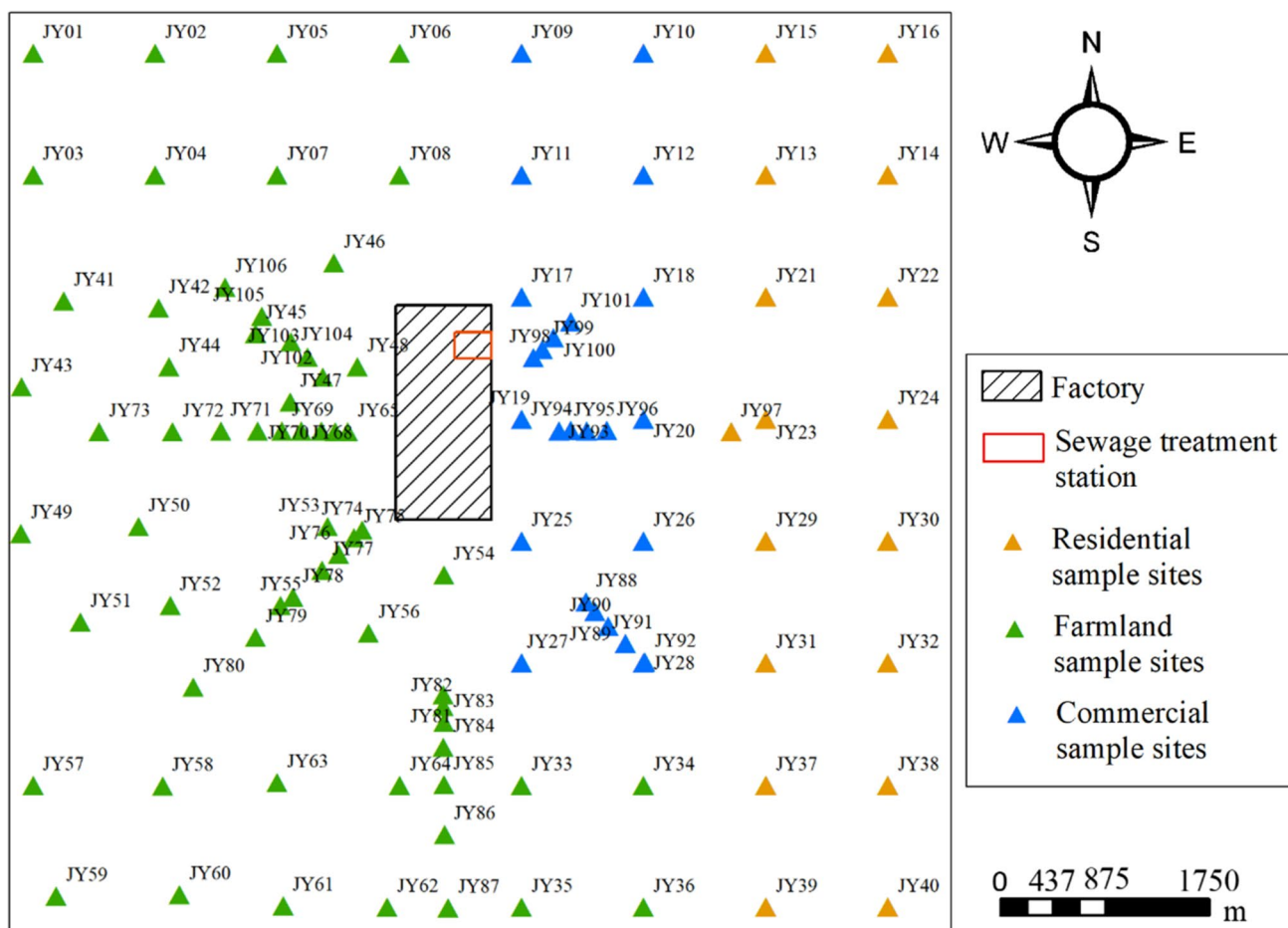
Fig. 1 Locations of the soil sampling sites and the factory

contamination. After removing stones and other debris, all soil samples were air dried at 20 °C and then passed through a 2.0 mm nylon sieve (Wang et al. 2019b) and sent to the laboratory for analyses.

The samples of Pb, Zn, Cu, Cr, Ni, Fe, Mn were digested in crucible by HNO_3-HF-$HClO_4$ digestion and analyzed by atomic absorption spectrometry (AAS). The samples of As were digested by HCl-HNO_3, and were analyzed by hydride generation atomic fluorescence spectrometry (HG-AFS). Using geochemical standard soil samples provided by the National Certified reference Materials Research Center to ensure quality assurance and quality control (QA/QC), and the recoveries of each element were between 88 and 106%. In addition, duplicate samples were determined for 25% of the collected samples, and the relative standard deviations were less than 5%.

Geo-accumulation Index (I_{geo})

Geo-accumulation Index (I_{geo}) can be used to evaluate the pollution level of heavy metals in soil (Al-Haidarey et al.

2010). The calculation principle of I_{geo} were described in the Text S1.

Positive Matrix Factorization (PMF) Model

The PMF model is a data analysis method based on the principle of factor analysis, which was proposed by Paatero and Tapper (1993). The calculation principle and expression of PMF were described in the Text S2.

Self-Organizing Map (SOM)

SOM is an unsupervised competitive learning neural network method. It builds its own network structure by simulating the response of human brain neurons to external stimuli, which can make a cluster area form near each best matching neuron, so that the input vectors of similar features are classified into a cluster. Heuristic rules can be used to select the appropriate number of neurons, such as $5\sqrt{n}$ suggested by Vesanto et al. (2000), where n is the number of samples. The Davies-Bouldin index can be used to determine the optimal

number of clusters (Wang et al. 2017). Kohonen (1982) proposed the SOM algorithm and introduced the specific implementation process of the algorithm. The specific steps contained in the algorithm were described in the Text S3.

Potential Ecological Risks Assessment

Potential ecological risks assessment results show the toxicological effects of heavy metals and environmental responses (Eq. (1)) (Hakanson 1980).

$$R_l = \sum E_r^i = \sum \frac{C_n^i}{B_r^i} \times T_r^i \tag{1}$$

R_l is the total potential ecological risks of all metals, E_r is the potential ecological risk of a single metal, C_n is the concentration of the metal, B_r is the environmental background value of a certain metal, and T_r is the toxicity coefficient of a certain metal. The toxicity parameters of Pb, As, Zn, Cu, Cr, Fe, Mn, and Ni were 5, 10, 1, 5, 2, 1, 1, 5, respectively (Hakanson 1980; Johnbosco 2020).

The grading values of the potential ecological risk, proposed originally by Hakanson, were based on eight pollutants (PCB, Hg, Cd, As, Pb, Cu, Cr, and Zn) which were different from the pollutants in this study. In order to make the grading more accurate, the grading of Hakanson's was adjusted on the basis of the pollutants in this study according to the previous research results (Fernández and Carballeira 2001; Ma et al. 2011; Chen et al. 2018). The grading method of Hakanson's was based on the maximum toxicity coefficient of pollutants and the total amount of toxicity coefficient of pollutants (Li et al. 2016). The adjustment of E_r is as follows: the first grade boundary value = non-pollution index $\left(\frac{C_n^i}{B_r^i} = 1\right) \times$ the maximum toxicity coefficient (T_r) among pollutants (10 for As in this study) = 10, and the grade value for each grade is 2 times higher than the last grade. For the adjustment of R_l, the unit grading value of toxicity coefficient (UGV) is determined first: UGV = 150 (first grade boundary value of Hakanson method)/133(total toxic coefficient of Hakanson method) ≈ 1.13. The total toxic coefficient of 8 pollutants in this study is 30, so the first grade boundary value = $30 \times 1.13 \approx 35$, and the grading value for each grade is 2 times higher than the last grade. The above adjustment method

has been proved to be a good way to describe potential ecological risks level (Chen et al. 2018). The comparison of the grading value between the Hakanson standard and this study was shown in Table 1.

Human Health Risks Assessment

Heavy metals can enter the human body through three ways: oral ingestion, oral and nasal inhalation, and skin contact. The average daily exposures (ADDs) for these three ways can be calculated by Eq. (2)–(4) (USEPA 1996; Praveena et al. 2015).

$$ADD_{ing} = \frac{C \times IngR \times EF \times ED}{BW \times AT} \times 10^{-6} \tag{2}$$

$$ADD_{inh} = \frac{C \times InhR \times EF \times ED}{PEF \times BW \times AT} \tag{3}$$

$$ADD_{dermal} = \frac{C \times SA \times AF \times ABS \times EF \times ED}{BW \times AT} \times 10^{-6} \tag{4}$$

The formula for calculating non-carcinogenic risk are (USEPA 1989):

$$HQ = \frac{ADI}{RfD} \tag{5}$$

$$HI = \sum HQ = \sum \frac{ADI}{RfD} \tag{6}$$

When HI < 1, it means that there is no non-carcinogenic risk to the human body. When HI > 1, it indicates that there is a non-carcinogenic risk to the human body, and the non-carcinogenic risk increases with the increase of HI (Qing et al. 2015). The formula for calculating carcinogenic risk is (Diami et al. 2016):

$$RI = \sum ADI \times SF \tag{7}$$

When the carcinogenic risk RI < 10^{-6}, the carcinogenic risk can be ignored; when 10^{-6} < RI < 10^{-4}, the carcinogenic risk is acceptable; when RI > 10^{-4}, the carcinogenic risk is unacceptable (Wu et al. 2015). The corresponding parameter values (IngR, EF, ED, BW, AT, InhR, PEF, SA, AF, ABS, RfD and SF) were summarized in the Table S1 and Table S2.

Table 1 Comparison of Hakanson classification standard in this study

E_r	Hakanson	< 40	40–80	80–160	160–320	> 320
	This study	< 10	10–20	20–40	40–80	> 80
R_l	Hakanson	< 150	150–300	300–600	> 600	–
	This study	< 35	35–70	70–140	140–280	> 280
Ecological risk level		Slight	Moderate	Strong	Quite strong	Extremely strong

Results and Discussion

Description Statistics of Heavy Metals in Topsoil

The statistical results were shown in Table 2. The average concentrations of the eight elements all exceeded the corresponding background values (CNEMC 1990), and the excess level in descending order was Pb > As > Cu > Zn > Ni > Cr > Mn > Fe. The excess levels of Mn, Ni, Cr, and Fe were lower, implying that they might be less affected by anthropogenic activities. The coefficient of variation from large to small was Pb > As > Cu > Zn > Cr > Mn > Ni > Fe. That is, the coefficient of variation of Pb, As, Zn, Cu concentrations were still ranked in the top four places, indicating that the spatial distributions of these four heavy metals had great variability. The mean contents of all heavy metals in the study area except Pb and As were lower than the corresponding criterion of the Chinese Environmental Quality Standard for Soils (CEPA 2018), which is used to measure the safety in farm produce and human health. However, the contents of Zn and Cu in a few of samples were over the criterion, and Pb, As, Zn, and Cu exceeded the criterion with excess rates of 92.5%, 67%, 1.9% and 5.7%, respectively, indicating that these elements may cause potential harm to safety of agricultural products and human health, therefore, a great attention should be paid to them.

Skewness values were applied to identify the heavy metals with normal or abnormal distribution. The heavy metals with skewness values between − 1 and 1 showed normal distribution and slightly positive skewness values of heavy metals were identified as abnormal (Chandrasekaran et al. 2015), and the skewness values of Pb, As, Zn, Cu in this study exceeded 1 (Table 2), which might indicating abnormal distribution of these four metals. And the histograms of the heavy metals could be seen in the Fig. S1.

In order to figure out the pollution level, the heavy metals were evaluated by the Geoaccumulation Index method (I_{geo}) (Table 2). 8.49% of Pb samples (the same below), 57.6% of As, 53.8% of Cu and 65.1% of Zn had I_{geo} values between 0 and 2, respectively; 65.1% of Pb, 19.8% of As and 1.89% of Cu had I_{geo} values between 2 and 4, respectively; and 25.5% of Pb had I_{geo} values greater than 4, and 4.72% of Pb had I_{geo} values greater than 5. The results showed that Pb, As, Zn, Cu caused pollution in different level, and Cr, Fe, Mn and Ni caused no pollution.

Source Identification of Heavy Metals in Topsoil

The PMF model identified three factors (Fig. 2), and residuals were between − 3 and 3. Coefficient of determination (R^2) between the measured and modeled concentrations of the models were all greater than 0.75, so it was appropriate to use this model to interpret the information contained in the initial data, and the results were reliable (Yang et al. 2013; Salim et al. 2019). Distribution maps of heavy metal concentrations in the study area which was used to explain the results obtained by PMF were shown in the Fig. S2.

The first factor, accounting for 41.3% of the total sources, was predominated by Pb, Zn, As, and Cu with the contributions of 68.8%, 49.2%, 43.3% and 54.5%, respectively. In the Fig. S2, Pb, Zn, As, and Cu all had large areas of high concentrations in the southeast and slowly decreased to the surroundings. As the elements of Zn, As, and Cu were major impurities in the lead ore (Li et al. 2010), so during the lead smelting process, industrial fume containing high concentrations of Pb, Zn, As, and Cu was generated. Industrial fume entered the atmosphere, and then reached the ground through dry deposition to increase the concentrations of heavy metals in the topsoil. The main wind direction of

Table 2 Summary of heavy metals concentrations in the topsoil around the factory

	Cr	Zn	Pb	Mn	As	Cu	Ni	Fe
Min (ppm)	41	64.9	51.2	269	7.9	20.4	31.7	21,800
Max (ppm)	101	328	2550	848	158	204	64	26,700
Mean (ppm)	69.3	140	584	606	45.3	49.4	39.1	24,600
CV (%)	14.7	36.8	84.8	21.6	72.5	65	12.1	5.1
Skewness	0.12	1.17	1.67	− 0.43	1.29	2.31	0.48	− 0.41
Kurtosis	0.65	1.42	2.77	− 1.02	1.15	7.08	− 0.26	− 0.26
Background value (ppm)[a]	63.8	60.1	19.6	574	11.4	19.7	26.7	24,300
Criterion (ppm)[b]	250	300	170	–	25	100	190	–
I_{geo}-mean	− 0.58	0.29	3.21	− 0.17	0.92	− 0.05	− 0.48	− 0.57
I_{geo}-max	− 0.03	1.6	5.79	0.35	3.07	2.21	− 0.16	− 0.45

CV Coefficient of variation

[a]Data from CNEMC (1990)

[b]Data from CEPA (2018)

Fig. 2 Factors profiles and source contributions of heavy metals from PMF model
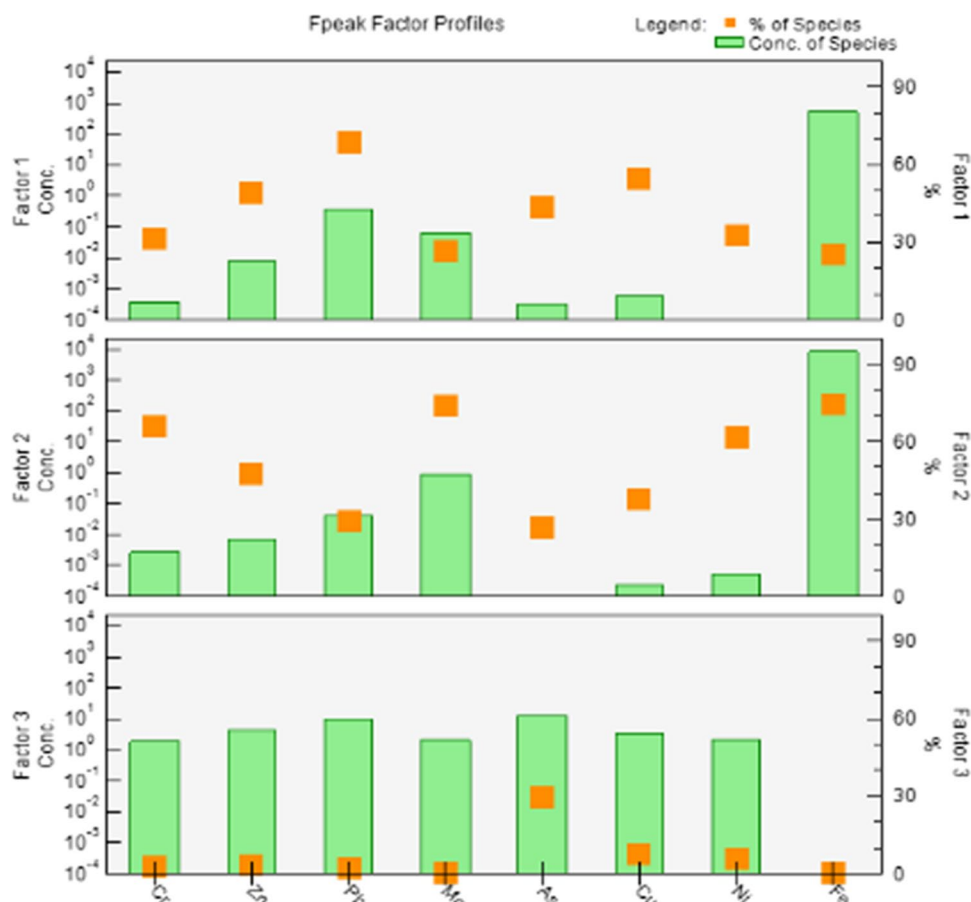
the study area was northwest wind, so the concentrations of Pb, Zn, As, Cu in the southeast of the factory were high, and the range of pollution plumes were extended in the southeast direction. Therefore, factor 1 represented the effect of industrial fume produced by the industrial activities of lead smelters on the heavy metals in topsoil.

The factor 2 (52.1%) was mainly associated with Fe (74.7%), Mn (73.6%), Cr (66.1%), and Ni (61.9%). Fe, Mn, Cr, and Ni in soil were often identified as natural sources of soil parent material, which has been confirmed in many studies (Huang et al. 2018b; Jiang et al. 2020). In the Fig. S2, the concentration distributions of Fe, Mn, Cr, and Ni had no obvious high-concentration region. And the concentrations of Fe, Mn, Cr, and Ni were close to the soil background values in the study area. I_{geo} of soil heavy metals also showed that these four elements did not cause pollution (Table 2). Therefore, Factor 2 was considered as a natural source of heavy metals of topsoil.

The load of As (29.8%) was the highest in factor 3 (6.6%). As shown in Fig. S2, in addition to a large area of high concentrations in the southeast, As had a small area of high concentrations in the northeast and the concentrations were even higher here. According to field investigation, the sewage

treatment station of the lead plant was located on the northeast of the plant. In 2017 and 2018, respectively, leakage occurred in the sewage treatment equipment and the sewage pipes, and only As in the sewage discharged by the lead plant exceeded relevant standards, and other elements were not, so that As-containing sewage entered the topsoil by this way. Therefore factor 3 represented the impact of wastewater leakage on the contents of heavy metals in topsoil.

Clustering of Sample Sites

Self-Organizing Map (SOM) was used to classify the sampling sites based on the concentrations of heavy metals. 50 (5 × 10) neurons and 4 clusters were selected according to Vesanto et al. (2000) and Davies–Bouldin index (Wang et al. 2017), and the results were shown in Fig. 3. The color gradients of Pb, Zn, and Cu neurons were consistent, indicating that the distributions of these three elements had a high similarity. Except for the difference of neurons color in the lower right corner, the color gradient of As in the other neurons was roughly the same as those of Pb, Zn, Cu. In addition, the neurons of Pb, Zn, Cu, and As in the first cluster were shown in dark blue, indicating low
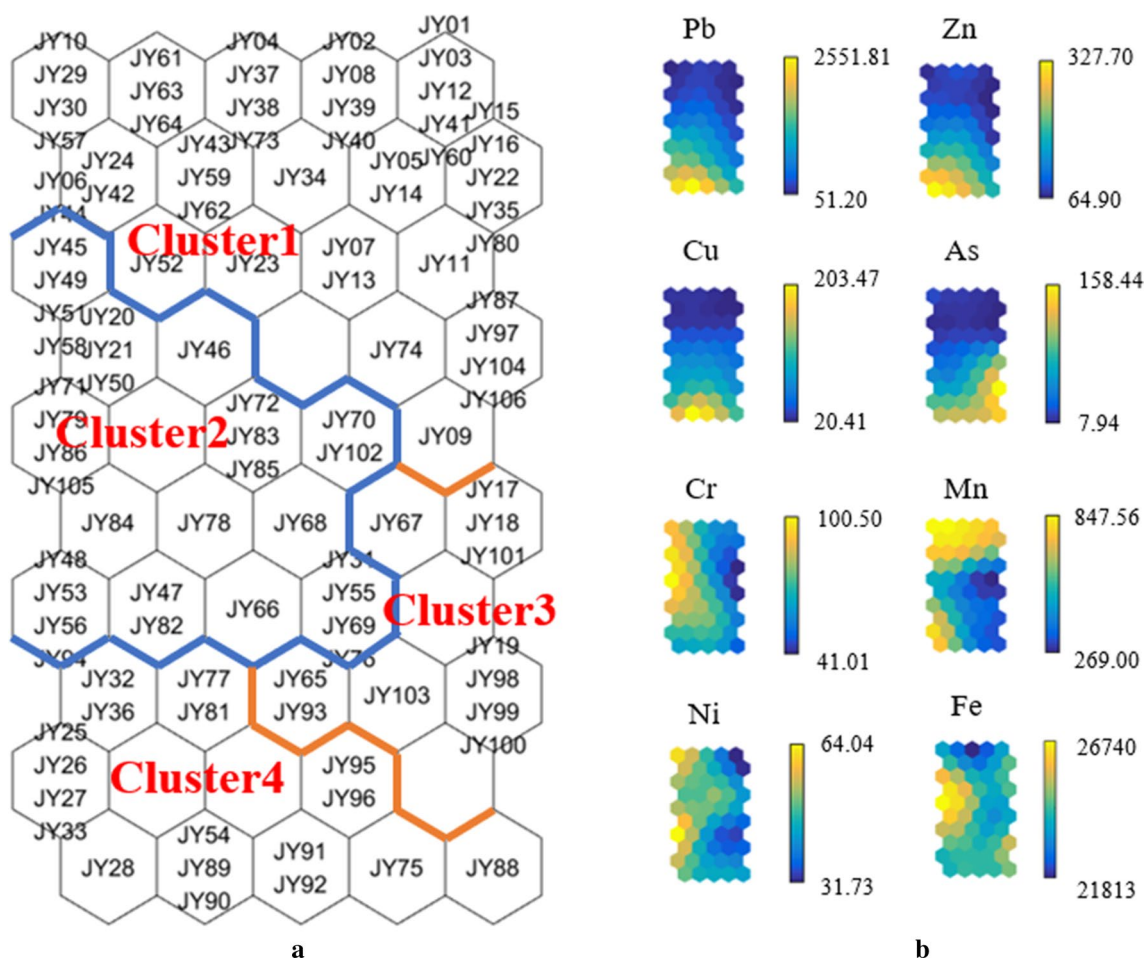
Fig. 3 The SOM results: **a** the clustering pattern in the SOM, the number in a hexagon denotes the sample number; **b** the SOM visualization of heavy metals, the numbers indicate values of the corresponding variables

concentrations of Pb, Zn, Cu, and As; the neurons of Pb, Zn, Cu, and As in the second cluster were all shown in light blue, suggesting that the concentrations of Pb, Zn, Cu, and As in this cluster were higher than those of the first cluster. The neurons color of Pb, Zn, and Cu in the third cluster were still light blue, but the neurons color of As were yellow, indicating that the concentrations of Pb, Zn, and Cu in this cluster were similar to those in the second cluster, but the concentrations of As were higher than those in the previous two clusters; The neurons color of Pb, Zn, and Cu in the fourth cluster were yellow, indicating that the concentrations of Pb, Zn, and Cu were the highest, and the neurons color of As were blue and yellow, which indicated that the concentrations of As in this group were also high but lower than those in the third cluster. The color gradients of Cr, Mn, Ni, and Fe had no obvious correlation with the clustering results, which were not the main reason for controlling clustering. The statistics of the heavy metal concentrations in these four clustering

results were shown in Table S3. The statistical results were consistent with the above analyses.

In combination with the results of PMF and SOM, it could be found that the first cluster of sampling sites were mostly located at a distance from the lead plant where the Pb, Zn, Cu and As concentrations were low, which could be regarded as the second source of PMF model results (natural source); the concentrations of As in the third cluster were the highest and the sampling sites were located at the northeast of the lead plant, which indicated that this cluster could be regarded as the third source (sewage leakage). The fourth cluster was distributed in the southeast, and the second cluster was distributed around factory other than the southeast. Under the influence of the prevailing northwest wind, the concentrations of the fourth cluster were higher than those of the second cluster. And under the influence of other direction winds, the concentrations of the second cluster were higher than those of the first cluster. As shown in the Fig. S2, southeast was not the only region where the heavy metals

concentrations increased. Thus, compared with the results of the PMF model, the SOM model identified the effect of wind direction on the distribution of heavy metals in topsoil in more details. The results of the SOM model could provide a basis for studying the potential ecological-health hazards caused by heavy metals in topsoil around the factory.

Ecological-Health Risks Assessment of Heavy Metals in Topsoil

Ecological Risks Assessment

As shown in Fig. 4, the ecological risks values (E_r) of all elements were below 10 (belong to the slight ecological risk) except Pb, As and Cu. As for Pb, E_r of 1 (1%) sampling site was lower than 10, which belonged to the slight ecological risk level; 10 (9%) sampling sites had the E_r of 10 to 20, which belonged to the moderate ecological risk level; 17 (16%) sampling sites had the E_r of 20 to 40, which belonged to the strong ecological risk level; 36(34%) sampling sites had the E_r of 40 to 80, which belonged to the quite strong ecological risk level; and 42 (40%) sampling sites had the E_r above 80, which belonged to the extremely strong ecological risk level. The E_r of As in 5 (5%) sampling sites were lower than 10, belonging to the slight ecological risk level; the E_r of As in 39 (37%) sampling sites were between 10 and 20, belonging to the moderate ecological risk level; the E_r of As in 30 (28%) sampling sites were between 20 and 40, belonging to the strong ecological risk level; the E_r of As in 25 (24%) sampling sites were between 40 and 80, belonging to the quite strong ecological risk level; the E_r of As in 7 (7%) sampling sites were higher than 80, belonging to the extremely strong ecological risk level. The E_r of Cu in 81

(76%) sampling sites were lower than 10, belonging to the slight ecological risk level; the E_r of Cu in 9 (8%) sampling sites were between 10 and 20, belonging to the moderate ecological risk level; the E_r of Cu in 7 (7%) sampling sites were between 20 and 40, belonging to the strong ecological risk level; the E_r of Cu in 9 (8%) sampling sites were between 40 and 80, belonging to the quite strong ecological risk level; No sample site of Cu was with the extremely strong level.

The E_r from large to small was: Pb > As > Cu > Ni > Cr > Zn > Mn > Fe, which was different from the order of heavy metals pollution degree (I_{geo}). This due to different ecotoxicity of different heavy metals. Heavy metals with very low pollution level, if the metal itself is highly toxic, it will still have a serious impact on the ecology. For example, the E_r of non-polluted Ni was higher than the E_r of contaminated Zn, which due to the high toxicity of Ni. In addition, as for the four heavy metals (Pb, As, Zn, Cu) with higher pollution level in 3.1, the risk values of As in the four clusters were ranked as: cluster III > cluster IV > cluster II > cluster I, and the risk values of Pb, Zn and Cu in the four clusters were all ranked as: cluster IV > cluster III > cluster II > cluster I, which were associated with pollution resulting from the As sewage leakage and the main wind direction.

For the total ecological risks (R_1), 16 (15%) sampling sites were with R_1 below 35 (slight ecological risk level); 8 (8%) sampling sites with R_1 between 35 and 70 (moderate ecological risk level); 37 (35%) sampling sites with R_1 between 70 and 140 (strong ecological risk level); 35(33%) sampling sites with R_1 between 140 and 280 (quite strong ecological risk level); 10 (9%) sampling sites with R_1 higher than 280 (extremely strong ecological risk level). From the total ecological risk distribution map (Fig. 5), the ecological risk value was high around the factory. And the high concentrations of Pb, Zn, Cu and As in the downwind direction of main wind formed highest ecological risks area. The ecological risks of Pb occupied the highest proportion in the area except the northeast part where As occupied the highest proportion because of sewage leakage. It was worth noting that the areas with the extremely strong ecological risk values (R_1 > 280) were mostly commercial land, only 1 sampling site with such risk value was located in the farmland. However, the areas with the quite strong ecological risks (140 < R_1 < 280) contained 23 sampling sites in the farmland, and the areas with strong ecological risks (70 < R_1 < 140) contained 18 sampling sites in the farmland. So, it was best to keep the farmland away from the factory and to monitor the heavy metals contents of the soil frequently to ensure the safety of the farm produce.
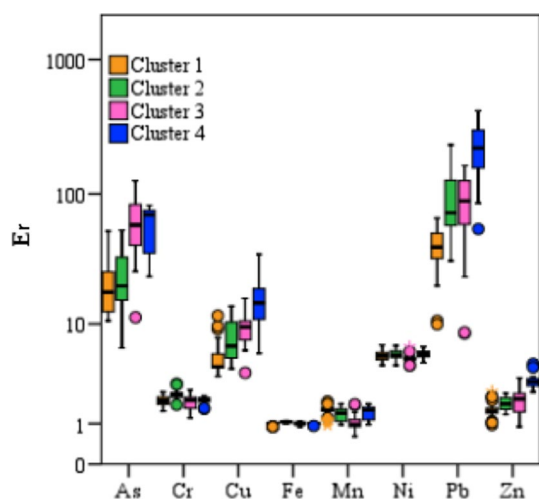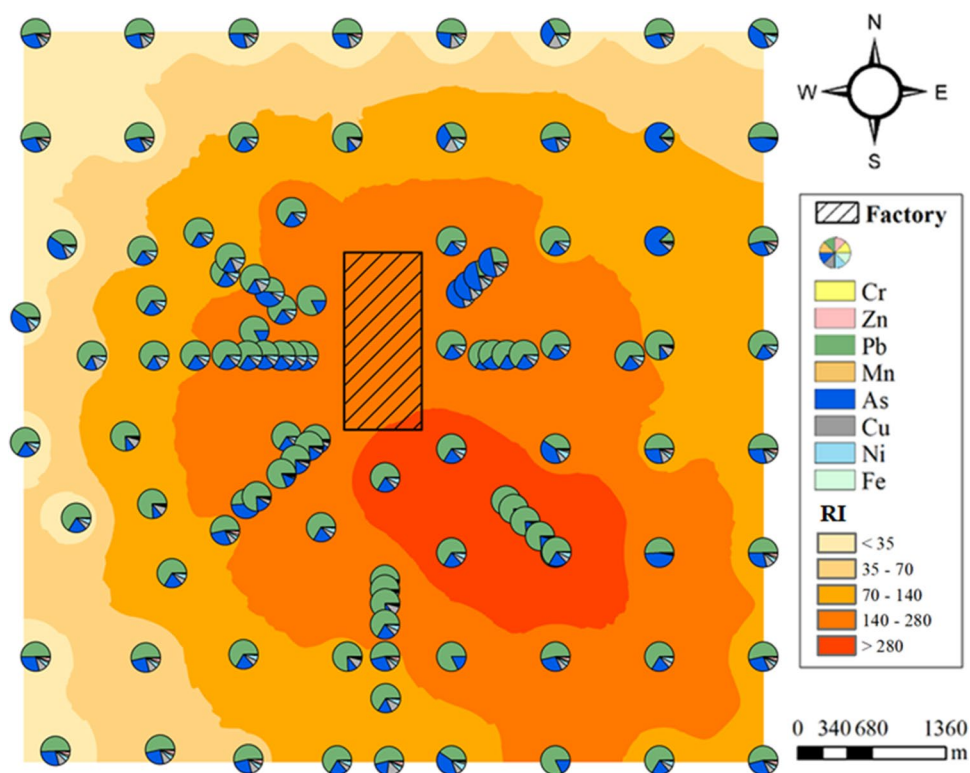

Fig. 4 Box drawing of potential ecological risks

Fig. 5 Spatial distribution of potential ecological risks

Table 3 Health risks of heavy metals in the topsoil of three exposure ways

	Non-cancer risk		Cancer risk	
	Adults	Children	Adults	Children
HQ_{ing}	4.87E−01	**2.29E+00**	5.42E−05	5.83E−05
HQ_{inh}	5.89E−04	5.49E−04	2.71E−07	5.54E−08
HQ_{dermal}	6.43E−02	3.16E−02	8.44E−07	7.30E−07

Data in this table are the average risk values of all samples caused by heavy metals

Human Health Risks Assessment

Heavy metals in the environment could enter human body through a variety of routes, specifically three ways: ingestion, dermal contact, and inhalation. As shown in Table 3 for the average risks, the level of risks to the human body caused by these three ways were in the following order: ingestion > dermal contact > inhalation. This result was consistent with those in the previous studies (Chabukdhara and Nema 2013; Men et al. 2018b; Wu et al. 2018b), and generally, these three ways caused negligible health risks or no health risks to human body, except non-carcinogenic risks to children through ingestion (highlighted in bold in Table 3). The health risks to children and adults caused by different heavy metals in each cluster were shown in Table 4. For non-carcinogenic risks, heavy metals individually showed no risks to adults. However, Pb in the second, third, and fourth clusters, and As in the third and fourth clusters caused potential risks to children (highlighted in bold in Table 4). Cluster IV accounted for the highest proportion of all sampling sites, indicating that children in the downwind direction of the factory might have higher non-carcinogenic risks compared with the other areas. For carcinogenic risks, all heavy metals posed negligible health risks or no health risks for both adults and children.

The health risks distribution maps (Fig. 6) showed the range of total health risks from heavy metals exceeding the standard (non-carcinogenic risk > 1; carcinogenic risk > 10^{-4}). Areas with high health risks were

Table 4 Health risks of heavy metals in the soils of each cluster

	Adults				Children			
	Cluster 1	Cluster 2	Cluster 3	Cluster 4	Cluster 1	Cluster 2	Cluster 3	Cluster 4
Non-cancer risk								
Cr	3.10E−02	3.60E−02	3.00E−02	3.10E−02	1.42E−01	1.68E−01	1.40E−01	1.44E−01
Zn	1.00E−03	1.00E−03	1.00E−03	1.00E−03	2.00E−03	3.00E−03	3.00E−03	5.00E−03
Pb	9.80E−02	2.23E−01	2.15E−01	5.44E−01	4.56E−01	**1.04E+00**	**1.00E+00**	**2.53E+00**
Mn	8.90E−02	7.90E−02	6.30E−02	8.20E−02	1.19E−01	1.05E−01	8.40E−02	1.10E−01
As	1.14E−01	1.37E−01	3.64E−01	3.41E−01	5.30E−01	6.37E−01	**1.70E+00**	**1.59E+00**
Cu	1.00E−03	2.00E−03	2.00E−03	3.00E−03	5.00E−03	7.00E−03	9.00E−03	1.60E−02
Ni	3.00E−03	3.00E−03	3.00E−03	3.00E−03	1.20E−02	1.30E−02	1.20E−02	1.30E−02
Percentage%	16.5	20.4	25.7	37.4	15	19.8	26.4	38.8
Cancer risk								
Cr	1.78E−05	2.11E−05	1.76E−05	1.81E−05	1.89E−05	2.23E−05	1.86E−05	1.91E−05
Pb	1.07E−06	2.44E−06	2.36E−06	5.96E−06	1.16E−06	2.63E−06	2.54E−06	6.42E−06
As	1.90E−05	2.29E−05	6.10E−05	5.71E−05	2.05E−05	2.46E−05	6.56E−05	6.14E−05
Ni	2.43E−09	2.52E−09	2.32E−09	2.49E−09	4.98E−10	5.16E−10	4.74E−10	5.09E−10
Percentage%	15.7	19.1	32.6	32.7	15.5	18.9	32.8	32.8

concentrated near the factory, and from the pie chart, Pb and As accounted for important proportion of the non-carcinogenic risks, and As accounted for an important proportion of the carcinogenic risks. The range of non-carcinogenic risks for adults was minimal, mainly in the southeast of the factory. The range of non-carcinogenic risks for children was large, almost covering the entire study area. The carcinogenic risks in the northeast were most serious for both adults and children, which were mainly affected by As sewage. Compared with adults, children were at higher health risks, and the uniqueness of their physiology, developmental stages and behavior leads to higher levels of exposure (NRC 2014). To effectively reduce children health risks, children should avoid the unhealthy habits of pica and allowing their fingers (Tan et al. 2016). Children could wear masks to prevent eating soil particles by mistake. In addition, fully understanding of the surrounding environment and meteorological conditions is necessary when outdoor public places such as parks and playgrounds are constructed. They should not be built in the vicinity of the plant sewage treatment station and the downwind of the factory.

Conclusions

This study evaluated the heavy metal pollution in the topsoil near a lead plant, central China. It was found that the topsoil was polluted by Pb, As, Cu, and Zn with varying degrees with the order of pollution level of Pb > As > Cu > Zn. And the heavy metals came from three sources: industrial fume emitted from the plant entering the topsoil through dry deposition (41.3%), natural sources of soil parent material (52.1%) and sewage leakage (6.6%). Under the influence of prevailing northwest wind, the ecological risks and health risks were high in the southeast of the factory, and the leakage of As-containing sewage caused high risks of carcinogenesis in the northeast of the factory. Therefore, priority should be given to ecological and health protection in the southeast and northeast of the factory. The data evaluation methods and results of the study may be useful to the soil pollution investigation and assessment in other areas.
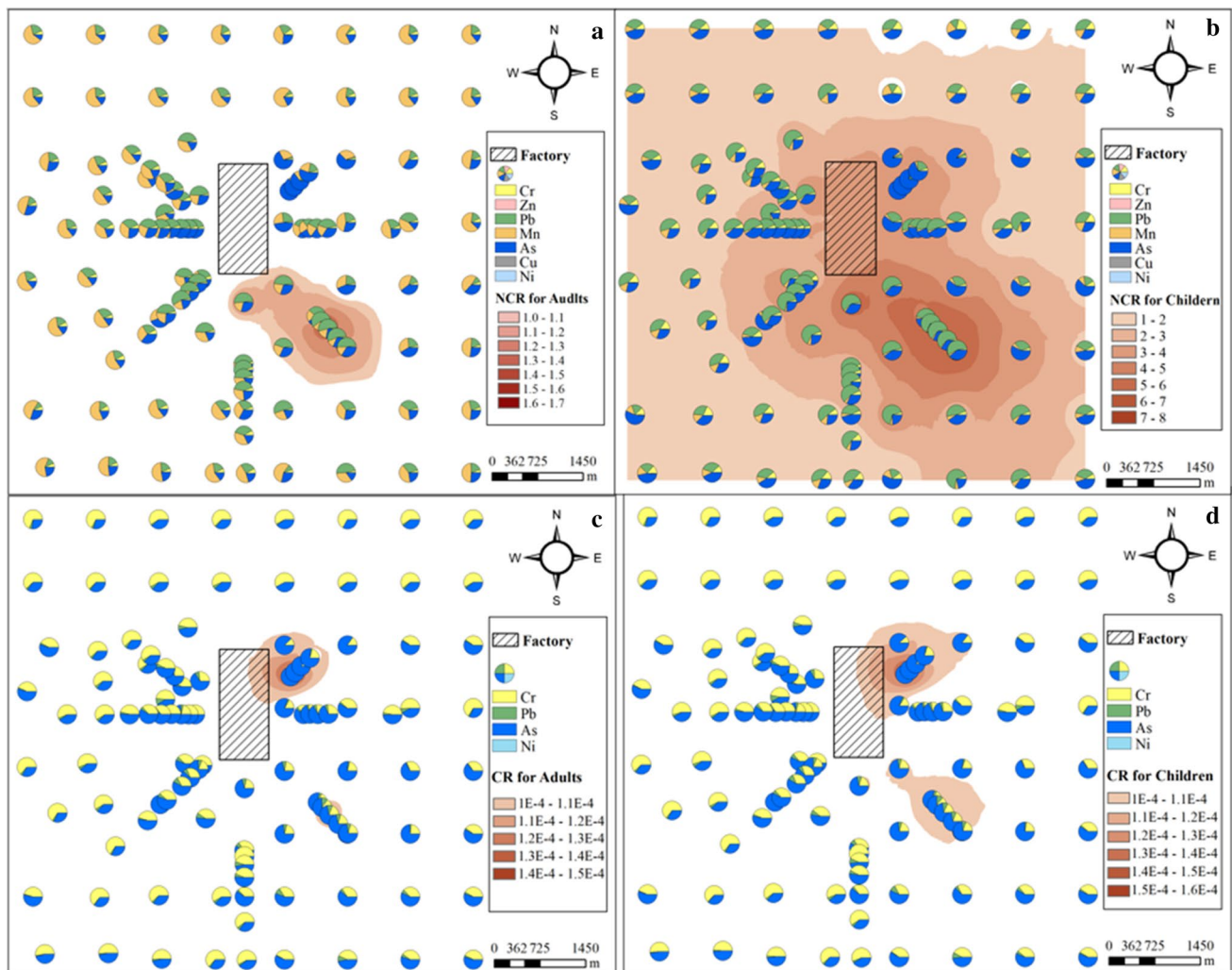
Fig. 6 Spatial distribution of human health risks (NCR: non-carcinogenic risk; CR: carcinogenic risk): **a** NCR for adults; **b** NCR for children; **c** CR for adults; **d** CR for children. Data used for interpolation are the sum of risk values from heavy metals for each sampling site

References

Al-Haidarey MJS, Hassan FM, Al-Kubaisey ARA, Douabul AAZ (2010) The geoaccumulation index of some heavy metals in al-hawizeh marsh. Iraq E-J Chem 7(s1):S157–S162

Ameh T, Sayes CM (2019) The potential exposure and hazards of copper nanoparticles: a review. Environ Toxicol Pharmacol 71:103220. https://doi.org/10.1016/j.etap.2019.103220

Antoniadis V, Golia EE, Liu Y, Wang L, Shaheen SM, Rinklebe J (2019) Soil and maize contamination by trace elements and associated health risk assessment in the industrial area of Volos, Greece. Environ Int 124:79–88. https://doi.org/10.1016/j.envint.2018.12.053

Astel A, Tsakovski S, Barbieri P, Simeonov V (2007) Comparison of self-organizing maps classification approach with cluster and principal components analysis for large environmental data sets. Water Res 41:4566–4578. https://doi.org/10.1016/j.watres.2007.06.030

Baitas H, Sirin M, Gökbayrak E, Ozcelik AE (2020) A case study on pollution and a human health risk assessment of heavy metals in agricultural soils around Sinop province, Turkey. Chemosphere 241:125015. https://doi.org/10.1016/j.chemosphere.2019.125015

Burges A, Epelde L, Garbisu C (2015) Impact of repeated single-metal and multi-metal pollution events on soil quality. Chemosphere 120:8–15. https://doi.org/10.1016/j.chemosphere.2014.05.037

Cai L, Wang Q, Wen H, Luo J, Wang S (2019) Heavy metals in agricultural soils from a typical township in Guangdong Province, China: Occurrences and spatial distribution. Ecotoxicol Environ Saf 168:184–191. https://doi.org/10.1016/j.ecoenv.2018.10.092

CEPA (Chinese Environmental Protection Administration) (2004) The technical specification for soil environmental monitoring (HJ/T 166-2004) **(in Chinese)**

CEPA (Chinese Environmental Protection Administration) (2018) Environmental quality standard for soils (GB15618-2018) **(in Chinese)**

Chabukdhara M, Nema AK (2013) Heavy metals assessment in urban soil around industrial clusters in Ghaziabad, India: probabilistic health risk approach. Ecotoxicol Environ Saf 87:57–64. https://doi.org/10.1016/j.ecoenv.2012.08.032

Chandrasekaran A, Ravisankar R, Harikrishnan N, Satapathy KK, Prasad MVR, Kanagasabapathy KV (2015) Multivariate statistical analysis of heavy metal concentration in soils of Yelagiri hills, Tamilnadu, India – spectroscopical approach. Spectrochim Acta A 137(137C):589–600. https://doi.org/10.1016/j.saa.2014.08.093

Chen Y, Jiang X, Wang Y, Zhuang D (2018) Spatial characteristics of heavy metal pollution and the potential ecological risk of a typical mining area: a case study in China. Process Saf Environ Prot 113:204–219. https://doi.org/10.1016/j.psep.2017.10.008

Cheng W, Lei S, Bian Z, Zhao Y, Li Y, Gan Y (2020) Geographic distribution of heavy metals and identification of their sources in soils near large, open-pit coal mines using Positive Matrix Factorization. J Hazard Mater 387:121666. https://doi.org/10.1016/j.jhazmat.2019.121666

CNEMC (China National Environmental Monitoring Centre) (1990) Soil elements background values in China. China Environmental Science Press **(in Chinese)**

Dai Z, Keating E, Bacon D, Viswanathan H, Stauffer P, Jordan A, Pawar R (2014) Probabilistic evaluation of shallow groundwater resources at a hypothetical carbon sequestration site. Sci Rep 4:4006. https://doi.org/10.1038/srep04006

Dai Z, Wolfsberg A, Reimus P, Deng H, Kwicklis E, Ding M, Ware D, Ye M (2012) Identification of sorption processes and parameters for radionuclide transport in fractured rock. J Hydrol 414–415:220–230. https://doi.org/10.1016/j.jhydrol.2011.10.035

Diami SM, Kusin FM, Madzin Z (2016) Potential ecological and human health risks of heavy metals in surface soils associated with iron ore mining in Pahang, Malaysia. Environ Sci Pollut Res Int 23:21086–21097. https://doi.org/10.1007/s11356-016-7314-9

Dong B, Zhang R, Gan Y, Cai L, Freidenreich A, Wang K, Guo T, Wang H (2019) Multiple methods for the identification of heavy metal sources in cropland soils from a resource-based region. Sci Total Environ 651(2):3127–3138. https://doi.org/10.1016/j.scitotenv.2018.10.130

Fernández J, Carballeira A (2001) Evaluation of contamination, by different elements, in terrestrial mosses. Arch Environ Contam Toxicol 40(4):461–468. https://doi.org/10.1007/s002440010198

Gülten YA (2011) Heavy metal contamination of surface soil around gebze industrial area. Turkey Microchem J 99(1):82–92. https://doi.org/10.1016/j.microc.2011.04.004

Hakanson L (1980) An ecological risk index aquatic pollution control. A sedimentological approach. Water Res 14:975–1001. https://doi.org/10.1016/0043-1354(80)90143-8

Han J, Huang Y, Zhong L, Zhao C, Cheng G, Huang P (2016) Adaptive protection scheme for microgrids based on SOM clustering technique. J Environ Manage 182:308–321. https://doi.org/10.1016/j.asoc.2020.106062

Harvey PJ, Rouillon M, Dong C, Ettler V, Handley HK, Taylor MP, Tyson E, Tennant P, Telfer V, Trinh R (2017) Geochemical sources, forms and phases of soil contamination in an industrial city. Sci Total Environ 584–585:505–514. https://doi.org/10.1016/j.scitotenv.2017.01.053

Hong YS, Rosen MR (2001) Intelligent characterisation and diagnosis of the groundwater quality in an urban fractured-rock aquifer using an artificial neural network. Urban Water 3:193–204. https://doi.org/10.1016/S1462-0758(01)00045-0

Hu W, Wang H, Dong L, Huang B, Borggaard OK, Bruun Hansen HC, He Y, Holm PE (2018) Source identification of heavy metals in peri-urban agricultural soils of southeast china: an integrated approach. Environ Pollut 237:650. https://doi.org/10.1016/j.envpol.2018.02.070

Huang J, Guo S, Zeng GM, Li F, Gu Y, Shi Y, Shi L, Liu W, Peng S (2018a) A new exploration of health risk assessment quantification from sources of soil heavy metals under different land use. Environ Pollut 243:49–58. https://doi.org/10.1016/j.envpol.2018.08.038

Huang J, Li H, Zeng G, Shi L, Gu Y, Shi Y, Tang B, Li X (2018b) Removal of Cd(II) by MEUF-FF with anionic-nonionic mixture at low concentration. Sep Purif Technol 207:199–205. https://doi.org/10.1016/j.seppur.2018.06.039

Jang E, Alam MS, Harrison RM (2013) Source apportionment of polycyclic aromatic hydrocarbons in urban air using Positive Matrix Factorization and spatial distribution analysis. Atmos Environ 79:271–285. https://doi.org/10.1016/j.atmosenv.2013.06.056

Jiang H, Cai L, Wen H, Hu G, Chen L, Luo J (2020) An integrated approach to quantifying ecological and human health risks from different sources of soil heavy metals. Sci Total Environ 701:1–8. https://doi.org/10.1016/j.scitotenv.2019.134466

Johnbosco CE (2020) Groundwater quality assessment using pollution index of groundwater (PIG), ecological risk index (ERI) and hierarchical cluster analysis (HCA): a case study. Groundwater Sustain Dev 10:1–8. https://doi.org/10.1016/j.gsd.2019.100292

Kim S, Kim TY, Yi SM, Heo J (2018) Source apportionment of PM2.5 using positive matrix factorization (PMF) at a rural site in Korea. J Environ Manage 214:325–334. https://doi.org/10.1016/j.jenvman.2018.03.027

Kohonen T (1982) Self-organized formation of topologically correct feature maps. Biol Cybern 43:59–69. https://doi.org/10.1007/BF00337288

Lang YH, Li GL, Wang XM, Peng P, Bai J (2015) Combination of unmix and positive matrix factorization model identifying contributions to carcinogenicity and mutagenicity for polycyclic aromatic hydrocarbons sources in liaohe delta reed wetland soils, China. Chemosphere 120:431–437. https://doi.org/10.1016/j.chemosphere.2014.08.048

Li F, Zhang J, Liu W, Liu W, Huang J, Zeng G (2018) An exploration of an integrated stochastic-fuzzy pollution assessment for heavy metals in urban topsoil based on metal enrichment and bioaccessibility. Sci Total Environ 644:649–660. https://doi.org/10.1016/j.scitotenv.2018.06.366

Li L, Cui J, Liu J, Gao J, Bai Y, Shi X (2016) Extensive study of potential harmful elements (Ag, As, Hg, Sb, and Se) in surface sediments of the Bohai Sea, China: sources and environmental risks. Environ Pollut 219:432–439. https://doi.org/10.1016/j.envpol.2016.05.034

Li L, Yao YS, Wang QL (2010) Determination of six elements in lead concentrate by inductively coupled plasma atomic emission spectrometry. Metall Anal 30(3):57–59

Li R, Cai G, Wang J, Ouyang W, Cheng H, Lin C (2014) Contents and chemical forms of heavy metals in school and roadside topsoils and road-surface dust of Beijing. J Soils Sediments 14(11):1806–1817. https://doi.org/10.1007/s11368-014-0943-z

Li S, Jia Z (2018) Heavy metals in soils from a representative rapidly developing megacity (SW China): levels, source identification and apportionment. CATENA 163:414–423. https://doi.org/10.1016/j.catena.2017.12.035

Li T, Sun G, Yang C, Liang K, Ma S, Huang L, Luo W (2019) Source apportionment and source-to-sink transport of major and trace elements in coastal sediments: combining positive matrix factorization and sediment trend analysis. Sci Total Environ 651(1):344–356. https://doi.org/10.1016/j.scitotenv.2018.09.19

Lischeid G (2009) Non-linear visualization and analysis of large water quality data sets: a model-free basis for efficient monitoring and

risk assessment. Stoch Environ Res Risk A 23:977–990. https://doi.org/10.1007/s00477-008-0266-y

Liu X, Shi H, Bai Z, Zhou W, Liu K, Wang M, He Y (2020) Heavy metal concentrations of soils near the large opencast coal mine pits in China. Chemosphere 244:125360. https://doi.org/10.1016/j.chemosphere.2019.125360

Lü J, Jiao W, Qin H, Chen B, Huang X, Kang B (2018) Origin and spatial distribution of heavy metals and carcinogenic risk assessment in mining areas at You'xi County southeast China. Geoderma 310:99–106. https://doi.org/10.1016/j.geoderma.2017.09.016

Lu X, Pan H, Wang Y (2017) Pollution evaluation and source analysis of heavy metal in roadway dust from a resource-typed industrial city in northwest china. Atmos Pollut Res 8(3):587–595. https://doi.org/10.1016/j.apr.2016.12.019

Ma J, Wang X, Hou Q, Duan J (2011) Pollution and potential ecological risk of heavy metals in surface dust on urban kindergartens. Geogr Res 30(3):486–495

Machender G, Dhakate R, Prasanna L, Govil PK (2011) Assessment of heavy metal contamination in soils around balanagar industrial area, Hyderabad. India Environ Earth Sci 63(5):945–953. https://doi.org/10.1007/s12665-010-0763-4

Men C, Liu R, Wang Q, Guo L, Miao Y, Shen Z (2018a) Uncertainty analysis in source apportionment of heavy metals in road dust based on positive matrix factorization model and geographic information system. Sci Total Environ 652:27–39. https://doi.org/10.1016/j.scitotenv.2018.10.212

Men C, Liu R, Xu F, Wang Q, Guo L, Shen Z (2018b) Pollution characteristics, risk assessment, and source apportionment of heavy metals in road dust in Beijing, China. Sci Total Environ 612:138–147. https://doi.org/10.1016/j.scitotenv.2017.08.123

Nakagawa K, Yu Z, Berndtsson R, Hosono T (2020) Temporal characteristics of groundwater chemistry affected by the 2016 Kumamoto earthquake using self-organizing maps. J Hydrol 582:124519. https://doi.org/10.1016/j.jhydrol.2019.124519

NRC (2014) A framework to guide selection of chemical alternatives. National Research Council, Washington, DC

Paatero P, Tapper U (1993) Analysis of different modes of factor analysis as least squares fit problems. Chem Intell Lab Syst 18(2):183–194. https://doi.org/10.1016/0169-7439(93)80055-M

Pareja-Carrera J, Mateo R, Rodríguez-Estival J (2014) Lead (Pb) in sheep exposed to mining pollution: Implications for animal and human health. Ecotoxicol Environ Saf 108:210–216. https://doi.org/10.1016/j.ecoenv.2014.07.014

Pathak AK, Yadav S, Kumar P, Kumar R (2013) Source apportionment and spatial–temporal variations in the metal content of surface dust collected from an industrial area adjoining Delhi, India. Sci Total Environ 443:662–672. https://doi.org/10.1016/j.scitotenv.2012.11.030

Pearce AR, Rizzo DM, Mouser PJ (2011) Subsurface characterization of groundwater contaminated by landfill leachate using microbial community profile data and a nonparametric decision-making process. Water Resour Res 47:W06511. https://doi.org/10.1029/2010WR009992

Pekey H, Karakaş D, Bakoğlu M (2004) Source apportionment of trace metals in surface waters of a polluted stream using multivariate statistical analyses. Mar Pollut Bull 49(9–10):809–818. https://doi.org/10.1016/j.marpolbul.2004.06.029

Praveena SM, Ismail SNS, Aris AZ (2015) Health risk assessment of heavy metal exposure in urban soil from Seri Kembangan (Malaysia). Arab J Geosci 8:9753–9761. https://doi.org/10.1007/s12517-015-1895-3

Qing X, Yutong Z, Shenggao L (2015) Assessment of heavy metal pollution and human health risk in urban soils of steel industrial city (Anshan), Liaoning, Northeast China. Ecotoxicol Environ Saf 120:377–385. https://doi.org/10.1016/j.ecoenv.2015.06.019

Salim I, Sajjad RU, Paule-Mercado MC, Memon SA, Lee BY, Sukhbaatar C, Lee CH (2019) Comparison of two receptor models PCA-MLR and PMF for source identification and apportionment of pollution carried by runoff from catchment and sub-watershed areas with mixed land cover in South Korea. Sci Total Environ 663:764–775. https://doi.org/10.1016/j.scitotenv.2019.01.377

Shang H, Wang W, Dai Z, Duan L, Zhao Y, Zhang J (2016) An ecology-oriented exploitation mode of groundwater resources in the northern Tianshan Mountains, China. J Hydrol 543(1):386–394. https://doi.org/10.1016/j.jhydrol.2016.10.012

Shi T, Zhang Y, Gong Y, Ma J, Wei H, Wu X, Zhao L, Hou H (2019) Status of cadmium accumulation in agricultural soils across China (1975–2016): from temporal and spatial variations to risk assessment. Chemosphere 230:136–143. https://doi.org/10.1016/j.chemosphere.2019.04.208

Skwarzec B, Kabat K, Astel A (2009) Seasonal and spatial variability of ^{210}Po, ^{238}U and $^{239+240}$Pu levels in the river catchment area assessed by application of neural network-based classification. J Environ Radioact 100:167–175. https://doi.org/10.1016/j.jenvrad.2008.11.007

Su Y, Chen W, Fan C, Tong Y, Weng T, Chen S, Kuo C, Wang J, Chang JS (2019) Source apportionment of volatile organic compounds (VOCs) by positive matrix factorization (PMF) supported by model simulation and source markers: using petrochemical emissions as a showcase. Environ Pollut 254:112848. https://doi.org/10.1016/j.envpol.2019.07.016

Tan SY, Praveena SM, Abidin EZ, Cheema MS (2016) A review of heavy metals in indoor dust and its human health-risk implications. Rev Environ Health 31:447–456

Tao S, Zhong B, Lin Y, Ma L, Zhou Y, Hou H, Zhao L, Sun Z, Shi H (2017) Application of a self-organizing map and Positive Matrix Factorization to investigate the spatial distributions and sources of polycyclic aromatic hydrocarbons in soils from Xiangfen County, northern China. Ecotoxicol Environ Saf 141:98–106. https://doi.org/10.1016/j.ecoenv.2017.03.017

Tchounwou PB, Yedjou CG, Patlolla AK (2012) Heavy metal toxicity and the environmen. EXS 101:133–164. https://doi.org/10.1007/978-3-7643-8340-4_6

USEPAS (1996) Soil screening guidance: technical background document. Superfund |US EPA

USEPA (1989) Risk assessment guidance for superfund. Hum Health Eval Manu A. vol. I (EPA/540/1-89/002)

Vesanto J, Himberg J, Alhoniemi E, Parhankangas J (2000) SOM toolbox for Matlab 5, report A57

Wang C, Lek S, Lai Z, Tudesque L (2017) Morphology of Aulacoseira filaments as indicator of the aquatic environment in a large subtropical river: the Pearl River, China. Ecol Indic 81:325–332. https://doi.org/10.1016/j.ecolind.2017.06.020

Wang M, Han Q, Gui C, Cao C, Liu Y, He X, He Y (2019a) Differences in the risk assessment of soil heavy metals between newly built and original parks in Jiaozuo, Henan Province. China Sci Total Environ 676(1):1–10. https://doi.org/10.1016/j.scitotenv.2019.03.396

Wang S, Cai L, Wen H, Luo J, Wang Q, Liu X (2019b) Spatial distribution and source apportionment of heavy metals in soil from a typical county-level city of Guangdong Province, China. Sci Total Environ 655:92–101. https://doi.org/10.1016/j.scitotenv.2018.11.244

Wen Y, Li W, Yang Z, Zhang Q, Ji J (2020) Enrichment and source identification of Cd and other heavy metals in soils with high geochemical background in the karst region, Southwestern China. Chemosphere 245:125620. https://doi.org/10.1016/j.chemosphere.2019.125620

Wongravee K, Lloyd GR, Silwood CJ, Grootveld M, Brereton RG (2010) Supervised self-organization maps for classification and determination of potentially discriminatory variables: illustrated

by application to nuclear magnetic resonance metabolomic profiling. Anal Chem 82:628–638. https://doi.org/10.1021/ac9020566

Wu J, Lu J, Li L, Min X, Luo Y (2018a) Pollution, ecological-health risks, and sources of heavy metals in soil of the northeastern Qinghai-Tibet Plateau. Chemosphere. https://doi.org/10.1016/j.chemosphere.2018.02.122

Wu S, Peng S, Zhang X, Wu D, Luo W, Zhang T, Zhou S, Yang G, Wan H, Wu L (2015) Levels and health risk assessments of heavy metals in urban soils in Dongguan, China. J Geochem Explor 148:71–78. https://doi.org/10.1016/j.gexplo.2014.08.009

Wu W, Wu P, Yang F, Sun D, Zhang DX, Zhou YK (2018b) Assessment of heavy metal pollution and human health risks in urban soils around an electronics manufacturing facility. Sci Total Environ 630:53–61. https://doi.org/10.1016/j.scitotenv.2018.02.183

Xiao T, Dai Z, Viswanathan H, Hakala A, Cather M, Jia W, Zhang Y, McPherson B (2017) Arsenic mobilization in shallow aquifers due to CO_2 and brine intrusion from storage reservoirs. Sci Rep 7(1):2763. https://doi.org/10.1038/s41598-017-02849-z

Xue JL, Zhi YY, Yang LP, Shi JC, Zeng LZ, Wu LS (2014) Positive Matrix Factorization as source apportionment of soil lead and cadmium around a battery plant (Changxing County, China). Environ Sci Pollut Res Int 21(12):7698–7707. https://doi.org/10.1007/s11356-014-2726-x

Yang B, Zhou L, Xue N, Li F, Li Y, Vogt RD, Cong X, Yan Y, Liu B (2013) Source apportionment of polycyclic aromatic hydrocarbons in soils of Huanghuai Plain, China: comparison of three receptor models. Sci Total Environ 443(15):31–39. https://doi.org/10.1016/j.scitotenv.2012.10.094

Ye C, Butler OM, Du M, Liu W, Zhang Q (2019) Spatio-temporal dynamics, drivers and potential sources of heavy metal pollution in riparian soils along a 600 kilometre stream gradient in Central China. Sci Total Environ 651(2):1935–1945. https://doi.org/10.1016/j.scitotenv.2018.10.107

Yuswir NS, Praveena SM, Aris AZ, Ismail SN, Hashim Z (2015) Health risk assessment of heavy metal in urban surface soil (Klang district, Malaysia). Bull Environ Contam Toxicol 95(1):80–89. https://doi.org/10.1007/s00128-015-1544-2

Zanotti C, Rotiroti M, Fumagalli L, Fumagalli GA, Canonaco F, Stefenelli G, Prévôt ASH, Leoni B, Bonomi T (2019) Groundwater and surface water quality characterization through positive matrix factorization combined with GIS approach. Water Res 159(1):122–134. https://doi.org/10.1016/j.watres.2019.04.058

Zelazny M, Astel A, Wolanin A, Malek S (2011) Spatiotemporal dynamics of spring and stream water chemistry in a high-mountain area. Environ Pollut 159:1048–1057. https://doi.org/10.1016/j.envpol.2010.11.021

Zhang P, Qin C, Hong X, Kang G, Qin M, Yang D, Pang B, Li Y, He J, Dick RP (2018a) Risk assessment and source analysis of soil heavy metal pollution from lower reaches of Yellow River irrigation in China. Sci Total Environ 633:1136–1147. https://doi.org/10.1016/j.scitotenv.2018.03.228

Zhang X, Wei S, Sun Q, Wadood SA, Guo B (2018b) Source identification and spatial distribution of arsenic and heavy metals in agricultural soil around Hunan industrial estate by Positive Matrix Factorization model, principle components analysis and geo statistical analysis. Ecotoxicol Environ Saf 159:354–362. https://doi.org/10.1016/j.ecoenv.2018.04.072

Zheng M, Salmon LG, Schauer JJ, Zeng L, Kiang CS, Zhang Y, Cass GR (2005) Seasonal trends in pm 25 source contributions in Beijing, China. Atmos Environ 39(22):3967–3976. https://doi.org/10.1016/j.atmosenv.2005.03.036

Zhou X, Wang X (2019) Impact of industrial activities on heavy metal contamination in soils in three major urban agglomerations of China. J Cleaner Prod 230(1):1–10. https://doi.org/10.1016/j.jclepro.2019.05.098

Zhu G, Wu X, Ge J, Liu F, Zhao W, Wu C (2020) Influence of mining activities on groundwater hydrochemistry and heavy metal migration using a self-organizing map (SOM). J Cleaner Prod 257:120664. https://doi.org/10.1016/j.jclepro.2020.120664

Zhu HN, Yuan XZ, Zeng GM, Jiang M, Liang J, Zhang C, Yin J, Huang HJ, Liu ZF, Jiang HW (2012) Ecological risk assessment of heavy metals in sediments of Xiawan port based on modified potential ecological risk index. Trans Nonferrous Met Soc China 22(6):1470–1477. https://doi.org/10.1016/S1003-6326(11)61343-5